

# Towards a fully autonomous robotic system for detection and removal of surface defects in fiber glass panels

James Oubre \* William Ard \*\* Joshua Nguyen \*\*  
Corina Barbalata \*\*

\* Electrical Engineering and Computer Science Department, Louisiana State University, Baton Rouge, LA 70803 USA (e-mail: [joubr13@lsu.edu](mailto:joubr13@lsu.edu)).

\*\* Mechanical and Industrial Engineering Department, Louisiana State University, Baton Rouge, LA 70803 USA (e-mails: [ward2@lsu.edu](mailto:ward2@lsu.edu), [jngu114@lsu.edu](mailto:jngu114@lsu.edu), [cbarbalata@lsu.edu](mailto:cbarbalata@lsu.edu)).

**Abstract:** Wind blades for turbines are commonly manufactured from fiber glass. A last step in the manufacturing process of such blades is sanding of the surface to remove defects that occur during the process. This paper presents an autonomous robotic system performing sanding operations for surface defect removal in fiber glass panels. The proposed approach uses a collaborative robotic system equipped with a vision system. Surface defects are detected using traditional computer vision algorithms and a path planning strategy is designed that solves multi-goal and coverage path planning problems. The robotic system equipped with a specialized end-effector will autonomously perform sanding of the defected areas using a constant velocity control system. Experimental results are evaluated based on the accuracy of the defect detection and roughness measurements before and after the sanding process has been completed.

**Keywords:** intelligent systems, automation, robotic system, computer vision, cascade control

## 1. INTRODUCTION

For wind energy turbines, lightweight fiber glass blades represent the appropriate choice as they allow the turbine to spin efficiently and produce more energy compared to other types of blades. After the fiber glass parts have been manufactured, finishing operations, such as sanding, are performed to remove surface defects, provide an appropriate surface for painting processes, or improve the aesthetics of the part. Such operations have been mainly carried out manually by human operators, the outcome of the process being dependent on the worker's skills (Kalt et al. [2016]).

In the past few years, collaborative robots (cobots) have gained interest in the context of Industry 4.0, as they are safe to operate in the presence of human workers. Their primary uses in an industrial setting have been for tasks such as assembly, inspection, pick & place applications, and, more recently, they have been introduced for sanding and polishing applications. Nevertheless, for cobots to be able to autonomously remove surface defects using sanding, several challenges must be addressed. These include but are not limited to autonomous detection of the defected areas and planning strategies to remove such defects.

This paper presents a fully autonomous collaborative robotic system, Fig. 1, for sanding surface defects in

\* The authors would like to acknowledge financial support from NSF Award Number 2024795, "NRI: FND: Collaborative Mobile Manufacturing in Uncertain Scenarios"

fiber glass panels. The proposed architecture starts with a perception system to detect surface defects in fiber glass materials using an affordable RGB-D camera. The novelty of this paper comes from the integration of specialized sub-systems to realize the capability of autonomous detection and removal of surface defects in flat fiber glass panels. A path planning architecture for robotic

manipulators is designed that combines multi-goal path planning and coverage path planning. Experimental results with a UR5e robotic system sanding defected areas in fiber glass panels are used to evaluate the proposed system.

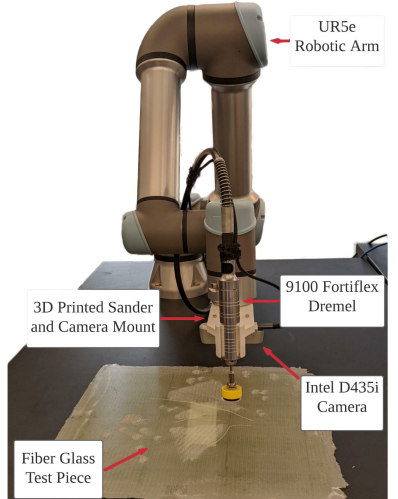


Fig. 1: Robotic system

## 2. BACKGROUND

This section presents a short background for defect detection, path planning approaches, and research previously done in the area of sanding and polishing using robotic systems.

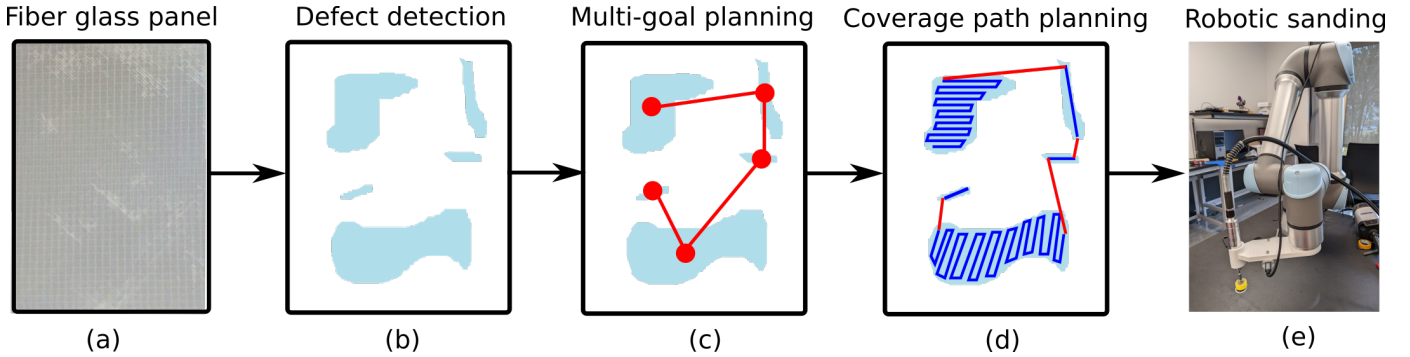


Fig. 2. Proposed approach: (a) Intel D435i mounted on the end-effector of the UR5e takes an image of the fiber glass panel; (b) a computer vision algorithm detects the surface defects in the panel; (c) a multi-goal path planning algorithm is used to ensure the robot will reach all defected areas; (d) a coverage path planning strategy is used to ensure complete damage removal (red lines represent end-effector travel in air, blue path represents end-effector path when in contact with the environment); (e) the UR5e executes the sanding only on the defected areas.

### 2.1 Surface defect detection in fiber glass

Many non-destructive testing (NDT) techniques, such as radiography, sheography, thermography and visual inspection, have been used in composite parts for defect detection (Tiwari and Raisutis [2018]). Visual based approaches have seen a significant rise in the past decade, focusing on both traditional visual inspection and data-driven approaches. However, one of the limitations of these techniques, is that they are dependent on the material properties and on the environmental medium.

The most common approaches for damage detection using visual inspection have focused on detecting edges, features, and regions. Filter-based approaches detect the intensity change in an image (Tiwari and Raisutis [2018]). A few examples worth mentioning are: Sobel filters, Canny edge detector, and Laplacian filters. Frequency based approaches, such as Gabor transform or the Optical Fourier transform have been used in fabrics for defect detection. Over the past few years, machine learning approaches, like convolutional neural networks (CNNs), have been extensively used in the area of defect detection (Chen et al. [2022]).

For fiber glass panels, visual inspection has been significantly less studied. Several papers have used active thermography for inspection of fiber glass. In (Souza et al. [2008]) the authors used an infrared camera with a heat source and perform Fast Fourier Transform (FFT) analysis on the obtained images to detect defects in adhesive joints. In (Muravsky et al. [2019]) the authors propose dynamic speckle patterns to detect subsurface defects with an RGB camera and a laser system.

### 2.2 Path planning for defect removal

Path planning for robotic systems performing sanding or polishing operations have been studied using an optimization framework based on the geometry of the part in (Chen et al. [2016]). The paper introduces the Hertz contact model for analyzing the contact between the tool and the surface to be polished. In (Kharidege et al. [2017]) a tool path planner is presented where the applied force and the polishing parameters are optimized. The planner is designed for complex shapes using a distribution of the area and scanning path method. A scanning path method is used in (Tam et al. [1999]), where paths are constructed on

a two-dimensional parametric plane and later are mapped on the 3D surface using the surface model. These papers have focused on the assumption that the entirety of the part must be sanded but this is not valid for defect removal in sanding applications.

Path planning for defect removal can be represented with two approaches: multi-goal path planning and coverage path planning. Multi-goal path planning is used to determine the best approach to navigate between defected areas, while coverage path planning (CPP) is used to determine a path that passes over all points in an area where a defect has been detected. The multi-goal path planning problem has been represented in the literature as the Traveling Salesman Problem (TSP) (Vicencio et al. [2014]). A heuristic approach based on genetic algorithms that results in a near-optimal solution is presented in (Sánchez and De la Rosa [2017]). Ant colony optimization is presented in (Tuani et al. [2017]) as a solution to the TSP. A sampling based solution based on multiple sampling trees is shown in (Janoš et al. [2021]). The Coverage Path Planning problem is related to the covering salesman problem (CSP), that represents a variation of the TSP. For the CSP, the agent must visit a neighborhood of the target area while for the CPP problem the agent must pass over all points in the target area. This is a computationally difficult problem whose complexity increases with the increase of dimensionality. In (Oksanen and Visala [2009]) an off-line trapezoid decomposition algorithm is presented for agricultural machines covering fields. An off-line grid based decomposition is presented in (Zelinsky et al. [1993]), while in (Gabriely and Rimon [2002]) an on-line approach, named Spiral-Spanning Tree Coverage algorithm for mobile robots is presented.

## 3. METHODOLOGY

The proposed pipeline for autonomous sanding of surface defects using cobots is shown in Fig. 2. The following paragraphs describe the details of each of these steps.

### 3.1 Surface defect detection in fiber glass

This project is focused on surface defects in fiber glass panels that are either visible (e.g. scratches, shape error, etc.) or palpable (e.g., crack, bump, etc.). The approach

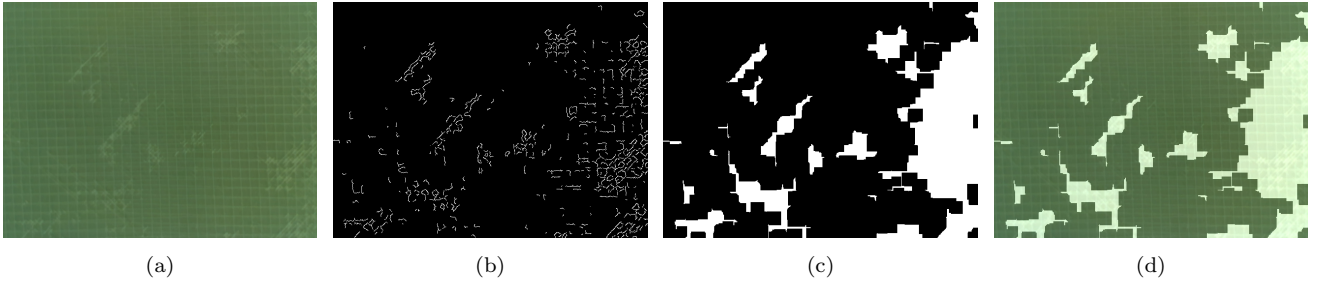


Fig. 3. Defect detection stages: (a) original image, (b) Canny edge detection, (c) morphological closing, (d) overlaid defect detection over original image

taken in this paper is part of the low-level processing methods where no prior knowledge about the content of the image is used.

The proposed algorithm utilizes traditional computer vision techniques such as canny edge detection, morphological closing, contour detection, and binary mapping. A flow diagram of the process can be seen in Fig. 3. First, an Intel D435i camera captures the RGB and depth images of the fiber glass sample. A canny edge detector is applied to the RGB image. This edge detector is chosen because of its high performance of detecting edges in a noisy image. This is vital for fiber glass panels as it successfully separates the inherit pattern visible underneath the surface of the fiber glass itself from the defects present on the surface. Through this method, scratches and surface roughness become apparent. To create a general region of the defective area, a morphological closing operation is applied. This merges nearby edges and fills openings within a certain area to create a blob like structure that correlates to the defective region on the sample. At this point, a binary image is generated with white pixels representing defective areas. Next, using topological analysis approaches, the individual blobs' contours are found and used to represent the different defective regions as arrays of pixels values. To remove false positive detected areas, a thresholding operation is performed to the regions previously extracted. The discrete arrays of pixels each represent a different region of defective surface and can then be input into the path planning algorithm. Although deep-learning has been widely used in computer-vision applications for defect detection and has been proven very successful, it still requires large amounts of data. As such, traditional computer vision methods have a clear advantages when limited data is available, and should be used when they provide a solution more efficiently (O'Mahony et al. [2019]).

### 3.2 Path planning for defect removal

Once the defects have been identified, the robot has to sand the indicated areas. This section presents the proposed approaches for the manipulator to navigate between various defected areas (multi-goal path planning) and the path taken in each of these areas to ensure its complete coverage (coverage path planning).

**Multi-goal path planning** The problem of navigating between various defected areas is represented as a TSP. The goal of the TSP is to find the shortest path that visits each node exactly once. The centroid of each of the defected areas represents the node that the robotic arm has to visit. A nearest neighbor algorithm is used to

create an initial path between nodes. A solution to the TSP is defined as a sequential set  $P$  that contains all nodes that must be visited, where  $P = [v_1, v_2, \dots, v_n]$ ,  $v$  represents a node, and  $n$  is the number of nodes that must be visited along a path. The length of the path is described as the sum of the 2-norm distance of one node to the next. The TSP is modeled as an optimization problem and the cost function chosen is defined as  $J = \sum_{i=1}^m E_i$ , where  $E_i$  represents the 2-norm distance from one node to the next. The 2-Opt heuristic approach (Ma et al. [2016]) has been chosen as the strategy for solving the TSP. This represents the most used local operator (Brodowsky et al. [2021]).

**Coverage path planning** Once a path between defected areas is generated, the next step is to create a coverage path planning strategy that ensures the entire defected area is covered. A grid-based sweeping algorithm for convex regions is proposed. The first step is to ensure that the defected areas have a convex representation. This is done using the Quickhull algorithm as presented in (Greenfield [1990]). For areas that overlap, a merging algorithm based on the union of the two defected regions is used. The next step is to design the grid-based decomposition. Cellular decomposition divides the space into non-overlapping polygons using boustrophedon decomposition. As these regions do not present any obstacles a lawnmower sweeping approach is used to cover the area with simple motions. The resolution of the sweeping algorithm is determined based on the sanding tool used to minimize overlapping between paths. At this stage, the multi-goal path and coverage planning are integrated, by replacing the centroid of each defected areas with the start of the lawnmower path for that corresponding defected zone. The robot is then commanded to travel in air to reach from one defected region to another. Once a defected area is reached the robot is required to make contact with the environment, applying a constant force while performing the sanding operation based on the coverage path.

## 4. RESULTS

**Experimental set-up:** To evaluate the results of the proposed pipeline, the UR5e robot is equipped with a custom tooling system consisting of the Intel D435i camera and the 9100 Fortiflex Dremel. The fiber glass panels used for testing are manufactured using vacuum-assisted resin infusion, each sample having a dimension of roughly  $230 \times 230$  mm, and presenting several surface defects such as scratches, roughness, and dry areas. The robot starts at a *home* position, ensuring that the camera is centered on the fiber glass. The camera then takes an image, the

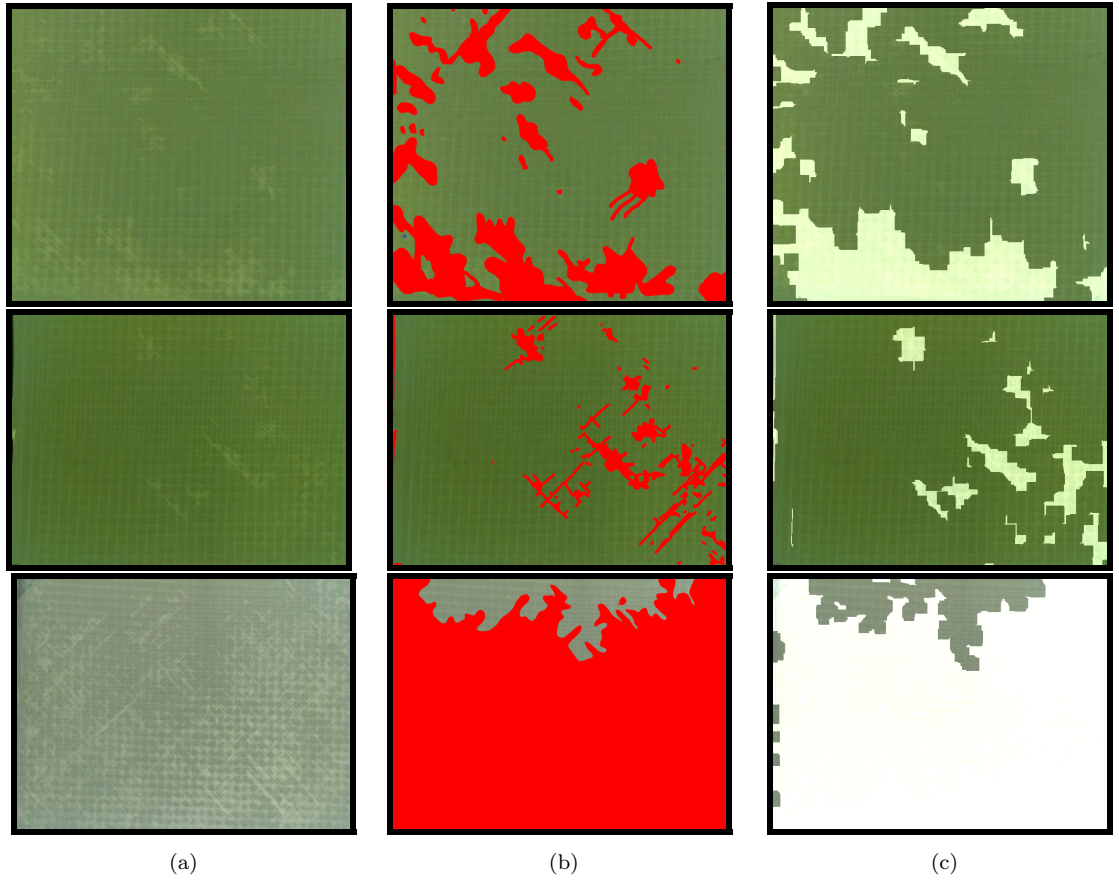


Fig. 4. Perception system results: (a) input image, (b) manually labeled image, and (c) automatic detection

defects are detected, and the paths are computed. The robot starts to move along these paths at a constant velocity of 0.1 m/sec and using a constant sander speed. The following paragraphs present the outcomes of the perception system and the sanding validation.

**Perception system evaluation:** The automatic defect detection results are compared with manually labeled samples, as can be seen in Fig. 4. The first column presents the input image taken by the Intel D435i, the manually labeled samples are shown in the second column, and the last column represents the automated detection. The proposed approach successfully detects the defected areas, this being confirmed by a quantitative evaluation presented in the following lines. Fifteen fiber glass panels have been used and the sensitivity, specificity, and accuracy of the detection is computed based on measurements of the number of pixels accurately and inaccurately detected. The averaged sensitivity obtained is 66.24% and the average specificity is 78.20% resulting in an accuracy of 81.02%.

The sensitivity of the image yields the rate at which true positives occur and the specificity the rate of true negatives. In this application, true positives and negatives are defined as pixels correctly characterized as defective or not. Furthermore, false positives and negatives represent pixels that are incorrectly characterized. These values indicate that the proposed approach has value for detection of surface defects in fiber glass samples and RGB data could be leveraged for detecting such defects. It should be noted that this process is sensitive to illumination changes. However, these sanding operations typically take place in

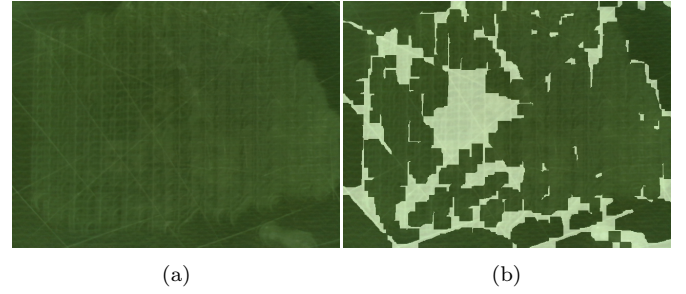


Fig. 5. Defect detection after sanding: (a) image after sanding took place, (b) defects detected in sample (a)

a controlled environment where lighting is consistent. Furthermore, the system was tested with fiber glass samples of different colors without affecting the performance of the system. In the last row of Fig. 4, the original color of the panel is significantly lighter compared to the previous samples. When overlaying the automatic detection over the original image, the defects are represented as white. This is just a visualization effect. Nevertheless, further research will be done to combat these conditions and make the system more robust. Fig. 5 shows the results of the perception system after the area has been sanded. These images indicate that if the damaged area has not been removed completely, the same perception system can be leveraged to detect the remaining defects and continue the sanding operation. This allows for a closed loop system where sanding of the area continues until the surface defect has been completely removed. These are promising results

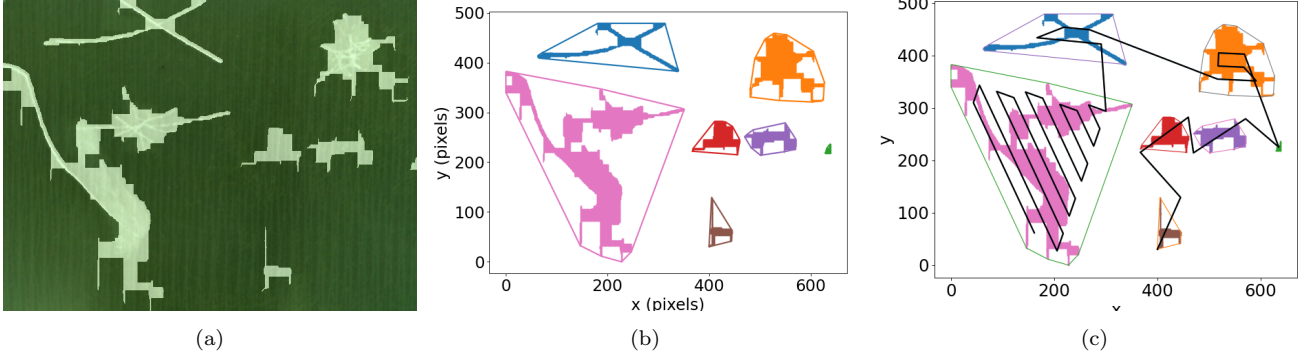


Fig. 6. Path planning when no overlapping of defected areas is present: (a) defects detected in fiber glass panel; (b) convex hulls established for each of the damaged areas; (c) multi-point path and coverage path merged together

for defect detection in fiber glass, but it also highlights that improvements to the current approach could be made by integrating higher end computer vision sensors and/or other image processing algorithms.

**Path planning results:** An example of the paths generated for the defected areas for both navigating between defected areas and ensuring full coverage of the defected areas is seen in Fig. 6. Once the defects have been detected, Fig. 6a, the convex hull is computed around these areas, Fig. 6b, and the multi-point path and coverage path are computed, Fig. 6c. In this case, a resolution consistent with the diameter of the sander, of 2.5 cm, was used for the coverage path planning. It can be seen that all defected areas have proper coverage and the navigation between different damaged areas is according to the minimum distance between damaged areas.

The end-effector path in Fig. 7 illustrates how the robot is moving to perform sanding over the damaged areas. To move among the defected regions, the end-effector lifts from the surface and travels in-air, hence the movement in the  $z$ -axis. Once the end-effector reaches an area that presents defects, it makes contact with the environment, applying a constant force of 4 Newtons in the  $z$ -direction, and follows the coverage path.

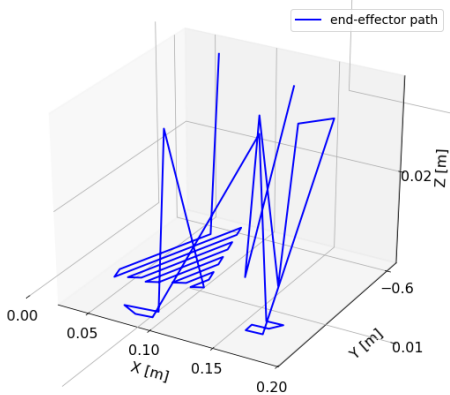


Fig. 7. End-effector trajectory for defects removal in Fig. 6

In Fig. 8 an example of coverage path planning is shown for the case when multiple defected areas marked with convex hulls overlap. Several convex hulls for areas that are connected are seen in Fig. 8b, and overlapping areas

are grouped together in Fig. 8c. For each of these areas a coverage path is determined, Fig. 8d. In this case, a resolution of 1.5 cm is used for coverage path planning. Fig. 8e shows the path to reach each of these areas. Because the navigation among different areas doesn't take into account where the coverage path planner starts and ends, the movement of the manipulator might not be optimal. This can be addressed by developing a more integrated cost function for the multi-goal path planning problem and it will be investigated in the future.

**Sanding evaluation:** To analyze the performance of the automated sanding procedure proposed in this paper, a comparison analysis of the surface roughness is performed before and after the robotic sanding procedure. To achieve this, a Mitutoyo Surface Roughness Tester has been used and 20 defected areas across 5 samples have been measured. All these areas have been detected and sanded by the robot. The metrics used to evaluate the roughness are  $Ra$  that is the average roughness in micrometers,  $Rq$  that is the root-mean-square roughness, and  $Rz$  representing the deepest ridge in micrometers. From Table 1 it can be seen that after employing the proposed approach with the cobot performing the sanding operation, the areas are significantly smoother, indicating that the surface defects have been reduced.

	$Ra [\mu m]$	$Rq$	$Rz [\mu m]$
Before sanding	4.55	6.29	26.19
After sanding	2.14	2.75	12.89

Table 1: Surface roughness measurements

## 5. CONCLUSIONS AND FUTURE WORK

This paper presents an autonomous robotic system performing sanding operations for surface defect removal in fiber glass panels. The proposed approach uses a collaborative robotic system equipped with a vision system. After the regions that contain the defects are detected and localized, a multi-goal path is designed to navigate among the detected regions, and a coverage path planning is leveraged to execute sanding. Classical approaches have been used, and have demonstrated the feasibility of having fully autonomous systems for defect detection and removal. Nevertheless, significant work can be done further to improve this initial study, such as using higher-end computer vision sensors, using more novel computer vision techniques, considering more integrated motion planning

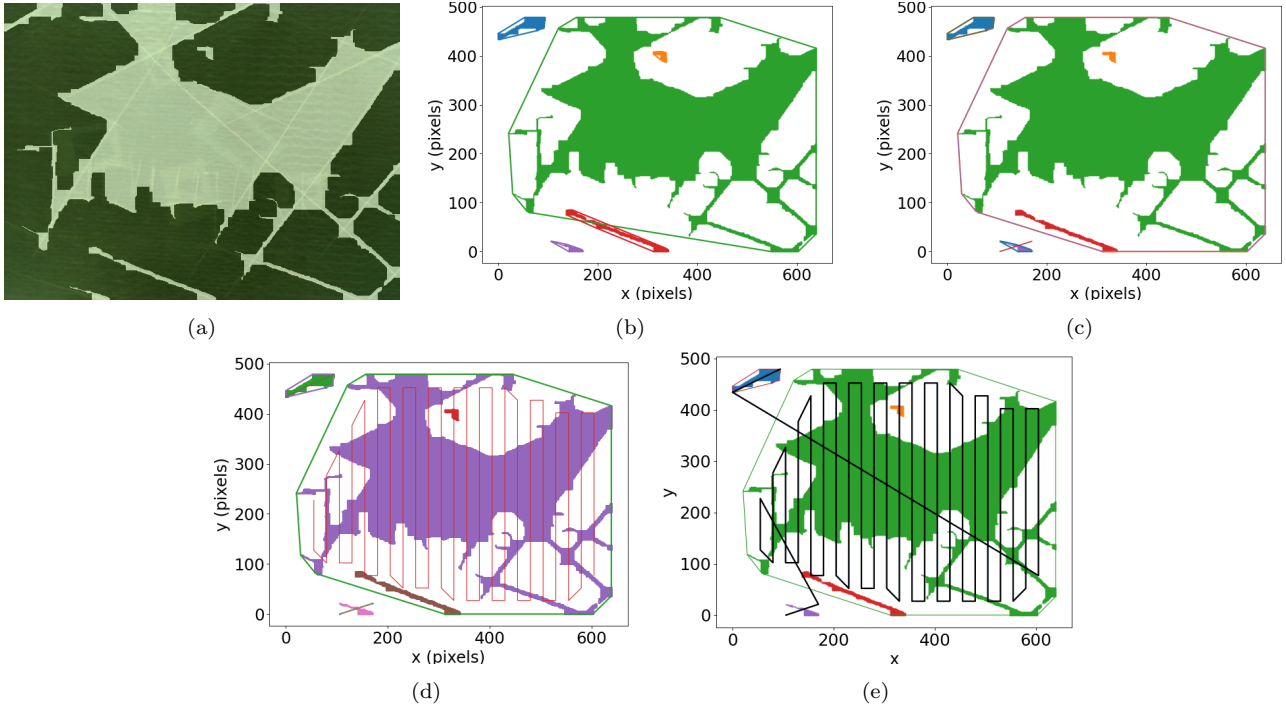


Fig. 8. Path planning when defected areas overlap: (a) defects detected in fiber glass panel; (b) convex hulls established for each of the damaged areas; (c) merged convex hulls of areas; (d) coverage path planning for each of the convex areas; (e) multi-point path and coverage path merged together

objectives, or investigating the importance of force and velocity regulation for obtaining for roughness decreasing. The team will continue to expand their findings and apply the proposed technology on curve surfaces.

#### ACKNOWLEDGEMENTS

The authors thank Dr. Genevieve Palardy and Chandler Lemoine for the support with fiber glass panels manufacturing, Donovan Gregg for manually labeling the samples, and Manuel Bailey for insights into the roughness measurements. The authors would like to acknowledge financial support from NSF #2024795, "NRI: FND: Collaborative Mobile Manufacturing in Uncertain Scenarios".

#### REFERENCES

Brodowsky, U.A., Hougardy, S., and Zhong, X. (2021). The approximation ratio of the  $k$ -opt heuristic for the euclidean traveling salesman problem. *arXiv preprint arXiv:2109.00069*.

Chen, B., Qi, J., and Hu, X. (2016). Polishing trajectory planning method based on the geometry and physics. In *IEEE International Conference on Information and Automation (ICIA)*, 1461–1466. IEEE.

Chen, M., Yu, L., Zhi, C., Sun, R., Zhu, S., Gao, Z., Ke, Z., Zhu, M., and Zhang, Y. (2022). Improved faster r-cnn for fabric defect detection based on gabor filter with genetic algorithm optimization. *Computers in Industry*, 134, 103551.

Gabriely, Y. and Rimon, E. (2002). Spiral-stc: An on-line coverage algorithm of grid environments by a mobile robot. In *Proceedings of IEEE International Conference on Robotics and Automation (Cat. No. 02CH37292)*, volume 1, 954–960. IEEE.

Greenfield, J.S. (1990). A proof for a quickhull algorithm. In *Electrical Engineering and Computer Science - Technical Reports*, volume 65.

Janoš, J., Vonásek, V., and Pěnička, R. (2021). Multi-goal path planning using multiple random trees. *IEEE Robotics and Automation Letters*, 6(2), 4201–4208.

Kalt, E., Monfared, R., and Jackson, M. (2016). Development of an intelligent automated polishing system.

Kharidege, A., Ting, D.T., and Yajun, Z. (2017). A practical approach for automated polishing system of free-form surface path generation based on industrial arm robot. *The International Journal of Advanced Manufacturing Technology*, 93(9), 3921–3934.

Ma, Z., Liu, L., and Sukhatme, G.S. (2016). An adaptive  $k$ -opt method for solving traveling salesman problem. In *IEEE 55th Conference on Decision and Control (CDC)*, 6537–6543. IEEE.

Muravsky, L., Kuts, O., Gaskevych, G., and Suriadova, O. (2019). Detection of subsurface defects in composite panels using dynamic speckle patterns. In *XI-th International Scientific and Practical Conference on Electronics and Information Technologies (ELIT)*, 7–10. IEEE.

Oksanen, T. and Visala, A. (2009). Coverage path planning algorithms for agricultural field machines. *Journal of field robotics*, 26(8), 651–668.

O'Mahony, N., Campbell, S., Carvalho, A., Harapanahalli, S., Hernandez, G.V., Krpalkova, L., Riordan, D., and Walsh, J. (2019). Deep learning vs. traditional computer vision. In *Science and Information Conference*, 128–144. Springer.

Sánchez, O.N.A. and De la Rosa, R.F. (2017). Path planning and following using genetic algorithms to solve the multi-travel salesman problem in dynamic scenarios. In *18th International Conference on Advanced Robotics*

(*ICAR*), 204–209. IEEE.

Souza, M., Rebello, J.M., Soares, S.D., and A., F.G. (2008). Defect detection in fiberglass reinforced epoxy composite pipes reproducing field inspection conditions. *9th International Conference on Quantitative InfraRed Thermography*.

Tam, H.y., Lui, O.C.h., and Mok, A.C. (1999). Robotic polishing of free-form surfaces using scanning paths. *Journal of Materials Processing Technology*, 95(1-3), 191–200.

Tiwari, K.A. and Raisutis, R. (2018). Identification and characterization of defects in glass fiber reinforced plastic by refining the guided lamb waves. *Materials*, 11(7), 1173.

Tuani, A.F., Keedwell, E., and Collett, M. (2017). H-aco: A heterogeneous ant colony optimisation approach with application to the travelling salesman problem. In *International Conference on Artificial Evolution (Evolution Artificielle)*, 144–161. Springer.

Vicencio, K., Davis, B., and Gentilini, I. (2014). Multi-goal path planning based on the generalized traveling salesman problem with neighborhoods. In *IEEE/RSJ International Conference on Intelligent Robots and Systems*, 2985–2990. IEEE.

Zelinsky, A., Jarvis, R.A., Byrne, J., Yuta, S., et al. (1993). Planning paths of complete coverage of an unstructured environment by a mobile robot. In *Proceedings of international conference on advanced robotics*, volume 13, 533–538. Citeseer.